Chemistry and Materials

The Center for Science Innovation

Research Article

Chem. Mater. 4 (2) 2025, 50-57

Potentiostatic Electrodeposition of FeCo Thin Films: Influence of Deposition Temperature and Saccharin Concentration

Arum Ayuningsih*

Department of Materials Science and Engineering, Chonnam National University, 300 Yongbong-dong, Buk-gu, Gwangju 61186, Republic of Korea

*Corresponding author: arumayu@jnu.ac.kr

Received
27 April 2025
Received in revised form
9 June 2025
Accepted
13 June 2025

DOI
https://doi.org/10.56425/rw1dv623

Abstract

The FeCo thin films were synthesized using a potentiostatic electrodeposition technique under varying deposition temperatures and saccharin compositions. The effects of these parameters on the film's crystallinity, composition, microstructure, and deposition behavior were systematically investigated. X-ray diffraction confirmed the formation of a single-phase FeCo structure under all conditions. Increasing the deposition temperature enhanced mass transfer and reduced anomalous codeposition behavior, as evidenced by the compositional shift toward higher cobalt content. The presence of saccharin was found to significantly influence the nucleation and growth processes through adsorption and the formation of metal–saccharinate complexes, which altered the deposition behavior. These results demonstrate that optimizing deposition parameters enables precise control over the composition and structure of FeCo thin films, which is crucial for the functional applications of magnetic and electrocatalysis.

Keywords: potentiostatic technique, electrodeposition, saccharin, thin film, FeCo

1. Introduction

Nanostructured FeCo alloy is a soft magnetic material with high saturation magnetization, making it suitable for various energy and electronic applications such as magnetoresistive RAM (MRAM), magnetic sensors, magnetostrictive actuators, etc [1–4]. FeCo also demonstrated high electrocatalytic performance, positioning it as a potential alternative to noble metal catalysts in hydrogen and oxygen evolution reactions [5–7].

These technologies require precise control over the material process, including thickness, structure, and compatibility with the application. The FeCo thin film can be fabricated at a nanometer scale, produced on a large scale, and easily miniaturized for modern technology. Among the available techniques, electrodeposition has emerged as an efficient and eco-friendly method for creating thin films. Electrodeposition offers numerous advantages, including low-cost operation, low-energy consumption, and the ability to form a homogeneous layer on complex surfaces [8–10]. Due to its controllability, electrodeposition is widely used in industries such as surface coating and electrode production. The choice of electrodeposition technique can significantly impact the properties of the thin film. It was reported that galvanostatic deposition produces smaller crystallite sizes and less compact layered structures than potentiostatic deposition [11]. However, using a potentiostatic approach helps achieve uniform growth due to better control over the deposition process, as it maintains a constant potential. It also leads to selective deposition, which minimizes side reactions and enables a specific targeted deposition [12]. Moreover, deposition behavior can be controlled by adjusting the electrical energy, resulting in a negative potential with less anomalous codeposition [13]. The quality and properties of electrodeposited films are highly dependent on deposition conditions, including the electric current, deposition temperature, and electrolyte conditions such as composition, pH, and additive agents. Therefore, the condition of the electrodeposition process was extensively studied.

A previous study confirmed that the deposition temperature significantly affects the composition and morphology of the FeCo thin film [14]. Qiang *et al.* [15] reported that the pH of the electrolyte bath can influence both the composition and grain size of FeCo thin film. The additive agent also has a crucial role in the electrodeposition process. For instance, the addition of an organic additive in the electrolyte bath can affect the ion adsorption mechanism during electrodeposition, which relates to the kinetic aspect of the process [16–18].

Besides influencing the film properties, these parameters also affect the performance of the electrodeposition process. It can be evaluated by observing its current efficiency and composition ratio. Deposition behavior was related to the kinetic process, which controlled the thin film composition and the design of the electrolyte bath. Particularly in the iron group (Fe-Co-Ni) alloy deposition, the codeposition of this group exhibits a phenomenon called anomalous codeposition [19]. This phenomenon will not occur according to the potential reduction standard, the reactive (less noble) metals are deposited more dominantly than the noble metals, as reported in some previous studies [19–23].

In this study, the effect of electrodeposition conditions, specifically the composition of the organic additive (saccharine) and deposition temperature, will be investigated on the production of FeCo thin films. The impact on the deposition process and FeCo thin film properties will be evaluated by determining the current efficiency, FeCo composition ratio, as well as the chemical composition, phase, and morphology of the resulting films.

2. Materials and Methods

2.1 Materials

The chemicals used were iron(III) sulfate heptahydrate ($FeSO_4 \cdot 7H_2O$), cobalt(II) sulfate heptahydrate ($CoSO_4.7H_2O$), boric acid (H_3BO_3), sodium saccharin ($C_7H_4NN_aO_3S$), and indium tin oxide-coated polyethylene terephthalate (ITO-PET).

2.2 Methods

2.2.1 Synthesis of FeCo

The electrolyte bath was prepared from their sulphate salt in boric acid conditions, the composition of which is shown in Table 1. The electrodeposited FeCo thin films were prepared using a potentiostatic technique at an applied cathodic potential of 1.0 V, which was controlled by an eDAQ EA163 potentiostat and e-corder 401. A three-electrode cell was used, with a platinum wire, Ag/AgCl, and a 20x10 mm ITO-PET (resistance 10 Ω/sq) serving as the counter electrode, reference electrode, and working electrode, respectively.

The effects of electrodeposition conditions were evaluated, including different variations of additive content (0-5g/L saccharin) and deposition temperature (0-50°C).

Table 1. Electrodeposition conditions and electrolyte composition.

Electrolyte composition	[mol/L]
$FeSO_4$	0.02
$CoSO_4$	0.08
H_3BO_3	0.4
time	30 minutes
pH	3.0
Saccharin	Variations

2.2.2 Characterizations

The thin film properties were investigated through a phase analysis and crystallization using an X-ray diffractometer (XRD, PANalytical Empyrean) with a 2θ range of 30°-100 ° in Cu Kα radiation (λ = 1.5406 Å) and a step size of 0.02 °. Additionally, the chemical composition was measured using an atomic absorption spectrometer (Shimadzu, AA-700), and the morphology was observed using a scanning electron microscope (Carl Zeiss, EVO MA10).

3. Results and Discussion

The potentiostatic electrodeposition method was used to deposit a FeCo thin film onto an ITO substrate under various parameters. The FeCo thin films obtained at different temperatures exhibit a single phase of the FeCo structure, wairute, identified as a cubic crystal structure with space group Pm–3 m, which is indexed to the XRD COD database code 9004229, reference code 96-900-4230. The diffraction peaks at approximately 2θ 44°, 66°, and 83° correspond to the (011), (002), and (112), respectively [23].

Figure 1a, however, shows that the intensity of these peaks varies with temperature, where the FeCo peak increases as the deposition temperature rises. Besides the peak shifting that occurred, the peak at 2θ 44° moves toward a higher 2θ value at 5 °C and 50 °C deposition temperatures. The optimum crystallite size of 41.47 nm was obtained at room temperature, while the lowest crystallite size of 19.35 nm was observed at 5 °C, as revealed in Fig. 1b.

The decreased temperature deposition could lead to the enhancement of overpotential. The elevated overpotential reduces the energy required for nucleus formation. Therefore, increasing the nucleation density (i.e., the number of nuclei per unit surface area), which in turn leads to smaller crystallite size [24].

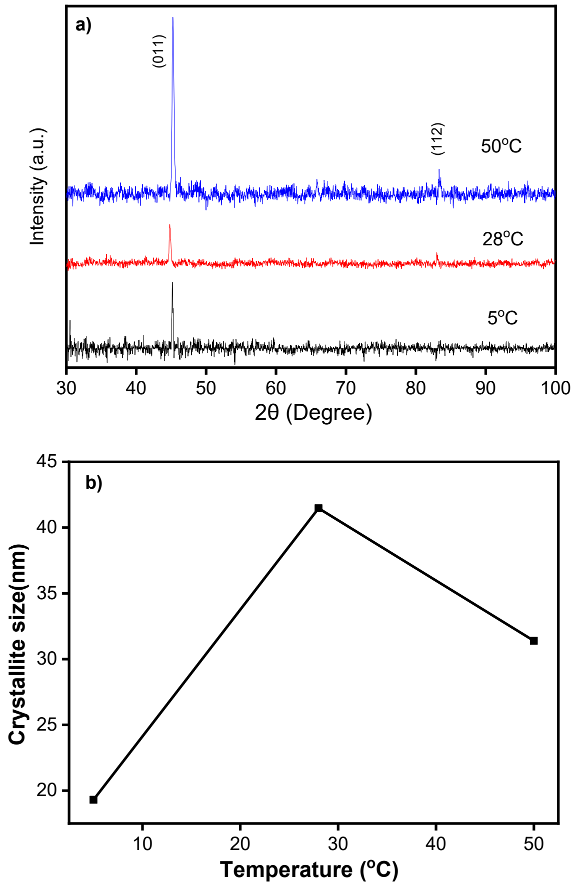

Figure 1. XRD pattern (a) and crystallite size (b) of FeCo thin films with 1 g/L of saccharin content deposited at different variations of temperatures.

Furthermore, the high deposition temperature of 50 °C also resulted in a decrease in crystallite size. This outcome relates to the kinetic driving force, which is enhanced at high temperatures. The increase in kinetic driving force is caused by the reduction in critical nucleus size, which approaches atomic dimensions, effectively eliminating the thermodynamic barrier for nucleation. Consequently, crystallite size is governed by kinetic factors, and according to the Arrhenius equation, the nucleation rate increases with temperature, leading to finer crystallites [25].

The micrographs exhibit an improvement in grain size with risen deposition temperature. Figures 2a and 2c show the effect of the presence of saccharin on the FeCo grain, which is deposited at room temperature. Comparing the two micrographs, the electrolyte bath without saccharin has a finer grain of FeCo than the one with 1 g/L saccharin addition. Although the FeCo grain was finer, the addition of saccharin in the electrolyte could improve the grain growth of FeCo, resulting in a denser microstructure with only minimal porosity observed in the micrograph. In the variation of temperature deposition with the addition of 1 g/L saccharin, the microstructure of FeCo exhibits a significant change in grain size and the formation of pores. The grain growth of FeCo was enhanced with increasing temperature deposition up to 50 °C, promoting the formation of larger grains.

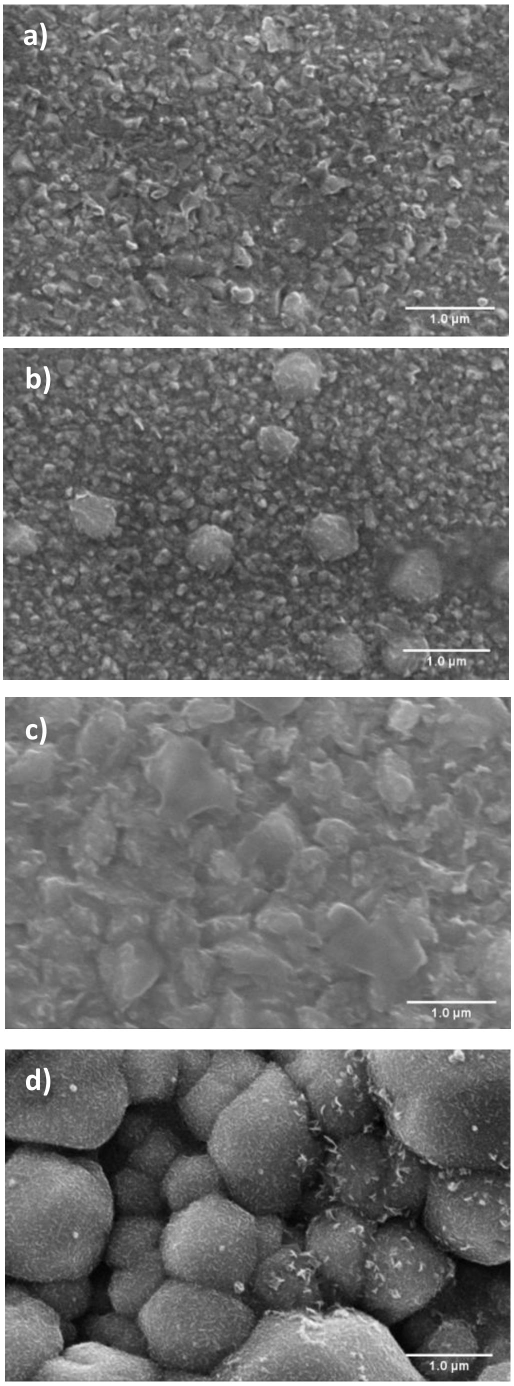

Figure 2. SEM micrograph of FeCo thin film with (a) 0 g/L saccharin at room temperature, and 1 g/L saccharin at deposition temperature (b) 5°C, (c) room temperature, and (d) 50°C.

Figure 2b indicates that the FeCo grain growth wasn't optimum at 5 °C, where the non-uniform grain of FeCo was formed. As the temperature deposition increased up to room temperature, the FeCo microstructure exhibited improvement, as evidenced by the formation of larger and more uniform grains with minimal porosity. The cavity expansion, however, was observed in the FeCo sample deposited at 50 °C, as shown in Fig. 2d. The increasing temperature deposition can enhance the energy and promote the hydrogen evolution reaction, which produces the hydrogen gas trapping and leads to porosity [19,26].

In the electrodeposition process, current efficiency and composition ratio are the primary indicators for evaluating the quality of the process and the properties of the thin film. Thus, the calculation of both indicators was necessary. The current efficiency is the ratio of the amount of thin film obtained to the theoretical value, which indicates the effectiveness of the current consumed during the electrodeposition process. Using equation 1 below, current efficiency can be calculated [23,27].

$$CE = \frac{w_j}{w_t} x100\% = \frac{w_j.F}{I.t} \sum \frac{c_i.n_i}{M_i} x100\% \qquad (1)$$

Where F is Faraday's constant, I is the applied current (ampere), and t is the electrodeposition time. Meanwhile, c_i, n_i, and M_i are the weight fraction of metal, the number of transferred electrons for one atom of metal that can be deposited, and the atomic mass of the metal, respectively. Since the iron group tends to have an anomalous codeposition behavior, to understand this behavior, the composition ratio of the metal in the thin film deposited should be calculated based on equation 2 below [20].

$$CRV = \frac{M\ wt\%\ in\ deposit}{M\ wt\%\ in\ electrolyte} \qquad (2)$$

The effect of temperature deposition on the performance of FeCo electrodeposition using a potentiostatic technique is shown in Fig. 1a. At a low temperature of 5°C, the current efficiency can reach around 89%, it was improved to 90% with the increased temperature where the optimum current efficiency of 90.9% was achieved at room temperature. The optimum trend can be explained using the transfer mass mechanism in the electrolyte. The increase in temperature deposition enhanced the solubility of electrolyte salts, which contributes to higher solution conductivity and accelerates the mass transfer of ions such as Fe^{2+}, Co^{2+}, and H^+ [28]. The improved conductivity and ion mobility facilitate a more efficient supply of metal ions to the cathode [29,30]. Thus, the deposition process on the substrate surface becomes more effective, resulting in increased current efficiency. However, an excessive increase in deposition temperature may also have adverse effects, one of which is the promotion of the hydrogen evolution reaction. This is attributed to the increased concentration of H^+ ions and the formation of metal monohydroxide complexes, which can lead to the generation of hydrogen gas [26]. Although the formation of these metal monohydroxide species may contribute to an increase in current efficiency, the hydrogen gas produced has the potential to hinder the nucleation of metal on the substrate surface [31].

Therefore, at high deposition temperatures, the current efficiency remains relatively high, as observed in this study, where a value of 90.12% was achieved. The reduction reactions of H^+ ions and water molecules involved in the hydrogen evolution process are described as follows [19].

$$2H^+ + 2e^- \rightarrow H_2 \qquad (3)$$
$$2H_2O + 2e^- \rightarrow H_2 + 2OH^- \qquad (4)$$

The composition ratio of Fe to Co exhibited an inverse trend with increasing deposition temperature: the Fe content decreased while the Co content increased. Although the Fe composition remained higher than that of Co at all temperatures, the difference between them narrowed significantly, indicating a reduction in anomalous codeposition behavior.

This trend is clearly illustrated in Fig. 3a, where the Fe composition in the deposited films decreases with increasing temperature, while the Co composition rises correspondingly. These were attributed to the enhanced supply of metal ions to the cathode with increasing deposition temperature. This condition leads to a higher diffusion coefficient and a greater concentration of metal ions within the electrical double layer [28,30]. The electrical double layer serves as a key region where metal ions accumulate before being reduced at the cathode. Therefore, controlling the deposition temperature significantly influences both the film composition and the deposition behavior.

Increasing the deposition temperature accelerates the mobility of metal ions, promotes the dissociation of metal–complex species, and enhances the desorption of monovalent iron species such as Fe^+(ads) and $FeOH^+$ from the substrate surface [28]. Consequently, monovalent iron species and iron–saccharin complexes that accumulate on the substrate tend to desorb, reducing iron incorporation into the film and favoring cobalt deposition [29].

This enhanced dissociation and desorption process reduces the iron deposition rate, thus diminishing the competitive deposition between Fe and Co. As a result, the cobalt deposition rate increases, leading to a reduction in anomalous codeposition. This is evident in the FeCo system, where the cathodic reduction value of Fe decreases with increasing temperature, whereas that of Co increases. The highest current efficiency and better microstructure of FeCo were obtained at room temperature.

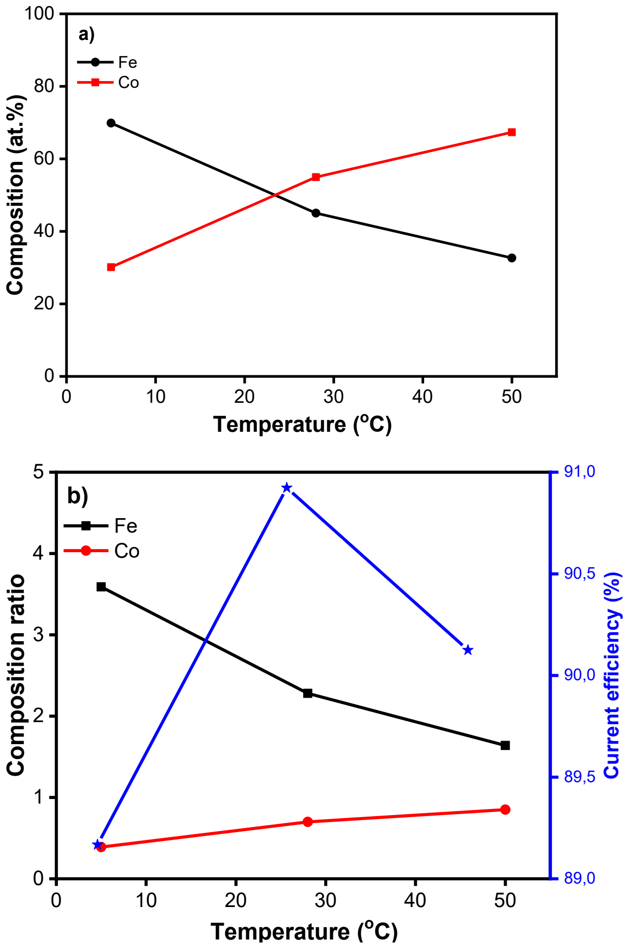

Figure 3. The chemical composition (a), the composition ratio value, and the current efficiency plot (b) of FeCo thin films in the different deposition temperatures.

The additive in the electrolytes plays a role in improving the quality of thin films. Inorganic additives primarily function through ion transport and electrochemical double-layer stabilization, which offer limited control over microstructure and deposit appearance. Organic additives provide finer control over the microstructure and appearance of the deposited layer. One of the most affordable organic additives is saccharin. Saccharin has a sulphonamide group in its structure, which can modify surface energy and refine grain formation, leading to finer, smoother, and more uniform metal thin films. Due to the sulphonamide group, saccharine causes the inclusion of sulphur in the deposit, which can form a passive layer. This passive layer on the surface can perform as a coating that enhances the corrosion resistance [17,32]. Hence, the optimization of saccharin composition in the preparation of FeCo thin films was investigated.

As shown in Figure 4a, the XRD pattern displays a single-phase FeCo, wairute, with no impurities, compared to the XRD COD database code: 9004229, reference code: 96-900-4230. The prominent diffraction peaks of FeCo appeared at 2θ = 45 ° (011), 66° (002), and 83° (112) [23]. The intensity of the diffraction peaks increased as the saccharin concentration increased up to 3g/L and decreased with higher amounts of saccharin composition. It is similar to the crystallite size; the addition of saccharin at 3g/L can achieve an optimum crystallite size of 65 nm.

The addition of saccharin in the electrolyte is believed to interfere with the interaction between metal ions and the cathode surface. In solution, saccharin exists as a negatively charged saccharinate ion, which competes with metal ions for adsorption on the substrate. Due to the bulky benzene ring in its structure, saccharinate ions are preferentially adsorbed onto the cathode surface, thereby hindering access for the smaller metal ions [33].

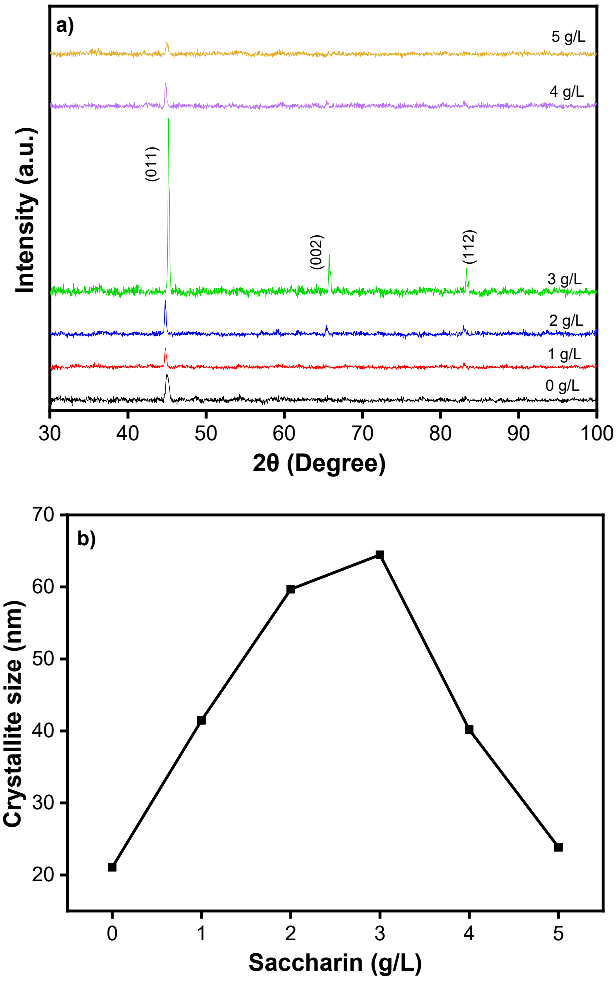

Figure 4. XRD pattern (a) and crystallite size (b) of FeCo thin films with different variations of saccharin contents deposited at room temperature

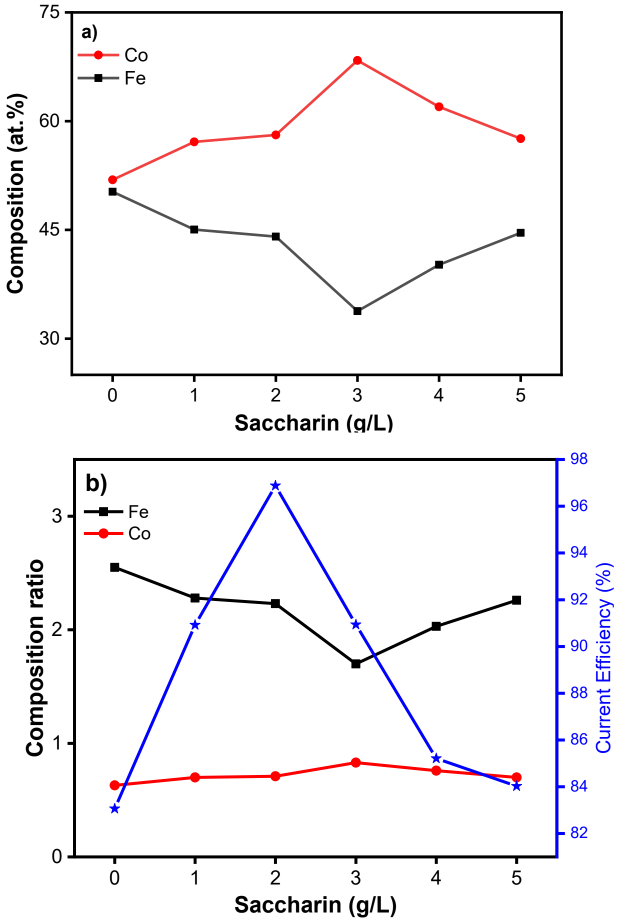

Figure 5. The Chemical composition (a), the composition ratio value, and the current efficiency plot (b) of FeCo thin films with different variations of saccharin contents deposited at room temperature.

During nucleation, the presence of saccharinate ions can inhibit the deposition of incoming metal ions through complex formation, allowing the initial nuclei more time and space to grow, which leads to larger crystallite sizes. However, at higher saccharin concentrations, the increase in negatively charged functional groups (O, S, and N atoms) enhances the interaction between metal ions and the cathode, accelerating nucleation [34].

Simultaneously, the accumulation of saccharinate ions on the substrate surface promotes the formation of metal-saccharinate complexes, which may block adion and adatom transport on the cathode. This process suppresses the growth of existing nuclei and encourages the formation of new nuclei, ultimately leading to crystallite size refinement [35].

The current efficiency achieved the optimum value of 96.8799% with the addition of 2 g/L saccharin. The addition of a small amount of saccharin (1-3 g/L) improved the current efficiency, with the CE value reaching above 90%. However, it declined drastically with 4 g/L saccharin, as shown in Fig. 5b. This decrease is attributed to the cathode-blocking mechanism of saccharin, which is related to the presence of the benzamide group [16,34]. Shirazi *et al.* [34] reported it was a product of saccharin desulfurization, with its negative charge delocalized over the N–C–O and N–C bonds, facilitating its adsorption onto the cathode surface. Besides the cathode-blocking mechanism, saccharin can also form a complex with the metal ion, which hinders the metal ion from depositing on the substrate. In addition to surface blocking, saccharin can also form complexes with metal ions, preventing their direct deposition on the substrate. This complexation process also influences the FeCo codeposition behavior. As previously mentioned, the electrodeposition was carried out at room temperature, where the anomalous codeposition behavior typically decreases. As shown in Fig. 5a, the cobalt content in the deposited films was consistently higher than that of iron. When comparing the elemental composition (Fig. 5a) with the composition ratio (Fig. 5b), it is evident that a near-unity composition ratio corresponds to a higher cobalt content and a lower iron content. This suggests that the addition of a small amount of saccharin (up to 3 g/L) reduces the anomalous codeposition behavior of FeCo.

Metal ions can form complexes with saccharin via either the nitrogen or sulfur atoms, with a stronger affinity typically observed at the nitrogen site due to more stable interactions [34]. Both Fe(II) and Co(II) can form octahedral complexes with two N-bonded saccharinate ligands in trans positions [36]. According to Costa et al., the redox behavior of Fe(II) and Co(II) saccharinate complexes exhibits significant differences. Fe(II)-saccharinate complexes exhibit two electrochemical pathways: a reversible oxidation of Fe(II) and an irreversible reduction of the saccharinate ligand. In contrast, only ligand reduction was observed in Co(II)-saccharinate complexes [37]. These differing behaviors may affect the deposition kinetics of Fe and Co during codeposition, which in turn impacts the deposition behavior and the chemical composition of FeCo thin films.

4. Conclusion

FeCo thin films were successfully deposited using a potentiostatic technique with controlled deposition temperatures and saccharin compositions. Both parameters significantly influenced the crystallite size, microstructure, chemical composition, and deposition behavior. Temperature variations affected the Fe/Co composition ratio by enhancing ion diffusion and altering redox kinetics, thereby reducing anomalous codeposition. The addition of saccharin improved deposition efficiency and modulated the codeposition behavior by forming metal-saccharinate complexes and modifying the adsorption dynamics at the cathode.

Author contributions

The author confirms sole responsibility for all aspects of the study, including conceptualization, methodology, investigation, data analysis, writing, and final approval of the manuscript.

Conflicts of interest

There are no conflicts to declare.

References

[1] R.H. Yu, S. Basu, L. Ren, Y. Zhang, A. Parvizi-Majidi, K.M. Unruh, J.Q. Xiao, High Temperature Soft Magnetic Materials: FeCo Alloys and Composites, 2000.

[2] T. Sourmail, Near equiatomic FeCo alloys: Constitution, mechanical and magnetic properties, *Prog Mater Sci*. **50** (2005) 816–880. https://doi.org/10.1016/j.pmatsci.2005.04.001.

[3] R.S. Sundar, S.C. Deevi, Soft magnetic FeCo alloys: Alloy development, processing, and properties, *International Materials Reviews*. **50** (2005) 157–192. https://doi.org/10.1179/174328005X14339.

[4] S. Gonçalves, V. Andrade, C.T. Sousa, J.P. Araújo, J.H. Belo, A. Apolinário, Tunable Iron–Cobalt Thin Films Grown by Electrodeposition, *Magnetochemistry*. **9** (2023). https://doi.org/10.3390/magnetochemistry9070161.

[5] W. Zhu, G. Zhu, C. Yao, H. Chen, J. Hu, Y. Zhu, W. Liang, Porous amorphous FeCo alloys as pre-catalysts for promoting the oxygen evolution reaction, *J Alloys Compd*. **828** (2020). https://doi.org/10.1016/j.jallcom.2020.154465.

[6] J.H. Park, S. Woo, J. Lee, H.Y. Jung, J.C. Ro, C. Park, B. Lim, S.J. Suh, Facile modified polyol synthesis of FeCo nanoparticles with oxyhydroxide surface layer as efficient oxygen evolution reaction electrocatalysts, *Int J Hydrogen Energy*. **46** (2021) 15398–15409. https://doi.org/10.1016/j.ijhydene.2021.02.027.

[7] X. He, R. Guo, Q. Zou, J. Yang, Z. Hu, L. Wu, Co-deposition of Co-Fe alloy catalysts for hydrogen evolution reaction based on ethylene glycol system, *Thin Solid Films*. **785** (2023). https://doi.org/10.1016/j.tsf.2023.140093.

[8] M.B. Kale, R.A. Borse, A. Gomaa Abdelkader Mohamed, Y. Wang, Electrocatalysts by Electrodeposition: Recent Advances, Synthesis Methods, and Applications in Energy Conversion, *Adv Funct Mater*. **31** (2021). https://doi.org/10.1002/adfm.202101313.

[9] I.M. Dharmadasa, J. Haigh, Strengths and Advantages of Electrodeposition as a Semiconductor Growth Technique for Applications in Macroelectronic Devices, *J Electrochem Soc*. **153** (2006) G47. https://doi.org/10.1149/1.2128120.

[10] A. Brenner, Electrodeposition of Alloys PRINCIPLES and PRACTICE, Academic Press, 1963.

[11] G.A.M. Ali, M.M. Yusoff, Y.H. Ng, H.N. Lim, K.F. Chong, Potentiostatic and galvanostatic electrodeposition of manganese oxide for supercapacitor application: A comparison study, *Current Applied Physics*. **15** (2015) 1143–1147. https://doi.org/10.1016/j.cap.2015.06.022.

[12] A. Nykiel, P. Ledwig, P. Pawlik, J. Ghanbaja, G. Cempura, A. Kruk, A. Walcarius, M. Kac, The influence of electrodeposition potential on the chemical composition, structure and magnetic properties of FeCoNi nanowires, *J Alloys Compd*. **982** (2024). https://doi.org/10.1016/j.jallcom.2024.173709.

[13] S. Budi, S. Muhab, A. Purwanto, B. Kurniawan, A. Manaf, Effect of the electrodeposition potential on the magnetic properties of FeCoNi films, *Materials Science- Poland*. **37** (2019) 389–394. https://doi.org/10.2478/msp-2019-0044.

[14] W. Lu, C. Ou, P. Huang, P. Yan, B. Yan, Effect of pH on the Structural Properties of Electrodeposited Nanocrystalline FeCo Films, 2013. www.electrochemsci.org.

[15] C. Qiang, J. Xu, S. Xiao, Y. Jiao, Z. Zhang, Y. Liu, L. Tian, Z. Zhou, The influence of pH and bath composition on the properties of Fe-Co alloy film electrodeposition, *Appl Surf Sci*. **257** (2010) 1371–1376. https://doi.org/10.1016/j.apsusc.2010.08.070.

[16] F. Lallemand, L. Ricq, M. Wery, P. Berçot, J. Pagetti, Kinetic and morphological investigation of CoFe alloy electrodeposition in the presence of organic additives, *Surf Coat Technol*. **179** (2004) 314–323.https://doi.org/10.1016/S0257-8972(03)00812-0.

[17] F. Lallemand, L. Ricq, M. Wery, P. Berçot, J. Pagetti, The influence of organic additives on the electrodeposition of iron-group metals and binary alloy from sulfate electrolyte, *Appl Surf Sci*. **228** (2004) 326–333. https://doi.org/10.1016/j.apsusc.2004.01.027.

[18] F. Lallemand, L. Ricq, E. Deschaseaux, L. De Vettor, P. Berçot, Electrodeposition of cobalt-iron alloys in pulsed current from electrolytes containing organic additives, *Surf Coat Technol*. **197** (2005) 10–17. https://doi.org/10.1016/j.surfcoat.2005.01.038.

[19] N. Zech, E.J. Podlaha, D. Landolt, Anomalous Codeposition of Iron Group Metals I. Experimental Results, 1999.

[20] S. Zhang, J. Yu, Z. Liu, Y. Yin, C. Qiao, Numerical and Experimental Investigation of the Effect of Current Density on the Anomalous Codeposition of Ternary Fe-Co-Ni Alloy Coatings, *Materials*. **15** (2022). https://doi.org/10.3390/ma15176141.

[21] S. Budi, S. Muhab, U. Cahyana, A. Purwanto, M. Paristiowati, TIME-DEPENDENT COMPOSITION OF THE ELECTRODEPOSITED NANOCRYSTALLINE Fe-Co-Ni FILMS, 2021.

[22] S. Budi, A. Manaf, The effects of saccharin on the electrodeposition of NiCoFe films on a flexible substrate, *Mater Res Express*. **8** (2021). https://doi.org/10.1088/2053-1591/ac1a2c.

[23] S. Budi, R.A. Tawwabin, U. Cahyana, Afriza, M. Paristiowati, Saccharin-assisted galvanostatic electrodeposition of nanocrystalline FeCo films on a flexible substrate, *Int J Electrochem Sci*. **15** (2020) 6682–6694. https://doi.org/10.20964/2020.07.74.

[24] W. Lu, P. Huang, K. Li, P. Yan, Y. Wang, B. Yan, Effect of Bath Temperature on the Microstructural Properties of Electrodeposited Nanocrystalline FeCo Films, 2013. www.electrochemsci.org.

[25] A.M. Rashidi, A. Amadeh, Effect of Electroplating Parameters on Microstructure of Nanocrystalline Nickel Coatings, 2010.

[26] M. Poroch-Seritan, I. Cretescu, C. Cojocaru, S. Amariei, C. Suciu, Experimental design for modelling and multi-response optimization of Fe-Ni electroplating process, *Chemical Engineering Research and Design*. **96** (2015) 138–149. https://doi.org/10.1016/j.cherd.2015.02.014.

[27] J.A.M. Oliveira, A.F. de Almeida, A.R.N. Campos, S. Prasad, J.J.N. Alves, R.A.C. de Santana, Effect of current density, temperature and bath pH on properties of Ni–W–Co alloys obtained by electrodeposition, *J Alloys Compd*. **853** (2021). https://doi.org/10.1016/j.jallcom.2020.157104.

[28] V. Zin, M. Dabalà, Temperature dependent properties and aggregation behaviour of FeCo nanoparticles produced sonoelectrochemically, *Journal of Nanoparticle Research*. **13** (2011) 7253–7262. https://doi.org/10.1007/s11051-011-0639-x.

[29] T.R. Lee, L. Chang, C.H. Chen, Effect of electrolyte temperature on composition and phase structure of nanocrystalline Fe-Ni alloys prepared by direct current electrodeposition, *Surf Coat Technol*. **207** (2012) 523–528. https://doi.org/10.1016/j.surfcoat.2012.07.069.

[30] O.K. Al-Duaij, M.M. Abou-Krisha, M.I. Attia, Influence of the deposition temperature on the electrodeposition mechanism of Zn-Co-Fe alloy, *Int J Electrochem Sci*. **12** (2017) 11972–11986. https://doi.org/10.20964/2017.12.62.

[31] L. Ricq, F. Lallemand, M.P. Gigandet, J. Pagetti, Influence of sodium saccharin on the electrodeposition and characterization of CoFe magnetic film, 2001.

[32] F. Lallemand, L. Ricq, P. Berçot, J. Pagetti, Effects of the structure of organic additives in the electrochemical preparation and characterization of CoFe film, 2002. www.elsevier.com/locate/electacta.

[33] A.C. Mishra, A.K. Thakur, V. Srinivas, Effect of deposition parameters on microstructure of electrodeposited nickel thin films, *J Mater Sci*. **44** (2009) 3520–3527. https://doi.org/10.1007/s10853-009-3475-y.

[34] S.M. Hassan Zadeh Shirazi, M.E. Bahrololoom, M.H. Shariat, The role of functional groups of saccharin in electrodeposition of nanocrystalline nickel, *Surface Engineering and Applied Electrochemistry*. **52** (2016) 434–442. https://doi.org/10.3103/S1068375516050112.

[35] S.H. Mosavat, M.E. Bahrololoom, M.H. Shariat, Electrodeposition of nanocrystalline Zn-Ni alloy from alkaline glycinate bath containing saccharin as additive, *Appl Surf Sci*. **257** (2011) 8311-8316.

https://doi.org/10.1016/j.apsusc.2011.03.017.

[36] E.J. Baran, V.T. Yilmaz, Metal complexes of saccharin, *Coord Chem Rev*. **250** (2006) 1980–1999. https://doi.org/10.1016/j.ccr.2005.11.021.

[37] B.S. Parajon Costa, E.J. Baran, Redox Behaviour of Divalent Metal Saccharinates, 1995.